THE MECHANICAL STRENGTH OF A BIPHASIC POLYCAPROLACTONE BONE SCAFFOLD FOR MEDIAL OPEN WEDGE HIGH TIBIA OSTEOTOMY IMPLANTATION

Oranich Tangniramai[1], Kowit Lounglaithong[3], Paweena Diloksumpan[2], Chris Charoenlap[3], and Phornphop Naiyanetr[1]*

[1]Department of Biomedical Engineering, Faculty of Engineering, Mahidol University of Thailand, Thailand
[2]Biofunctional materials and device research group, National Metal and Materials Technology Center, Thailand
[3]Department of Orthopedics Faculty of Medicine, Chulalongkorn University of Thailand, Thailand

ABSTRACT

Mechanical strength is a requirement of the bone scaffold for osteoarthritis treatment by the medial open wedge high tibia osteotomy (MOWHTO). *The mechanical compression of the scaffold which depends on material concentration and structure must be concerned in MOWHTO substitution due to help to prevent the delayed bone healing process from scaffold collapse. This study was divided into two sections: (i) the influence of varying concentrations between DBM-HA mixed PCL scaffold (20/80, 30/70, and 40/60 % wt./wt. DBM-HA/PCL) on compressive strength, and (ii) the compressive strength of the 0°-90° orientations DBM-HA/PCL scaffold (20/80% wt./wt.) constructed with 300-500 µm pore dimension by the extrusion-based bioprinting method. The results exhibited that the concentrations of DBM-HA/PCL affected mechanical properties in the scaffold. The low DBM-HA concentrations scaffold showed high compressive strength. The 20/80 % wt./wt. DBM-HA/PCL represented the 23.25 MPa and 157.63 MPa of compressive stress and modulus respectively. The 0°-90° orientations scaffold with 20/80 % wt./wt. DBM-HA/PCL showed the 2.90-16.03 MPa and 70.92 MPa of compressive stress and modulus. In conclusion, the mechanical compression of 20/80 % wt./wt. DBM-HA/PCL scaffold fabricated with 300-500 µm pore size has a range within tibia cancellous bone and it is suitable for an alternative bone in the MOWHTO.*

Keywords: bone scaffold, polycaprolactone, demineralized bone matrix, hydroxyapatite, mechanical strength, and open wedge high tibia osteotomy

Manuscript received on April 1, 2022; revised on May 15, 2022, accepted on May 25, 2022. *Corresponding author E mail: Phornphop.nai@mahidol.ac.th, Department of Biomedical Engineering, Faculty of Engineering, Mahidol University, Thailand.

1. INTRODUCTION

A bone defection with 10-14 mm is a critical problem following the correcting knee alignment for osteoarthritis with the medial open wedge high tibia osteotomy (MOWHTO) without bone graft surgery because there is a lack of bone formation and delayed bone union process. *[1-2]*. Normally, the minimum critical size of bone defection is greater than or equal to 4 mm leading to failure of osteogenesis *[3-4]*. Alternatively, adding a bone graft can promote the bone healing process in 3-8 months after substitution *[5-8]*. On the other hand, infective viral transmission disease, autoimmune rejection, and donor site morbidity are risk factors for implantation with grafting. Furthermore, the allograft cannot induce osteoinduction, which promotes bone-cell differentiation and is critical in osteogenesis *[9-10]*. Figure 1 illustrates the MOWHTO.

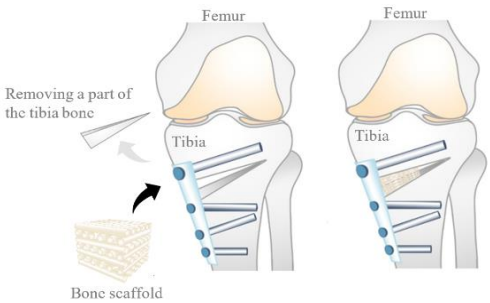

Figure 1. (a) Medial open wedge high tibia osteotomy (MOWHTO) and (b) Medial open wedge high tibia osteotomy with bone scaffold substitution

Newly technique, a bone scaffold which is an alternative synthetic bone was developed to risk factor reducing, bone defection preventing, and bone union improving. Therefore, the bone scaffold required biological and mechanical properties similar to the native bone. The osteogenesis scaffold should be constructed with biocompatible materials and appropriate architecture according to biological and mechanical properties. Earlier, the scaffold was fabricated with pure polycaprolactone (PCL) because of

its properties. The PCL is a synthetic biopolymer with a melting point of 60 degrees Celsius, which is higher than the melting point of human body temperature [11]. The PCL scaffold has been used in plastic surgery because of biocompatible, biodegradable, non-toxicity, and slow degradable [12-14]. Conversely, the PCL limitation is low compressive strength and non-favorable cell attachment. To improve osteogenesis, hydroxyapatite (HA) is added to the polymeric scaffold which is called the hybrid scaffold. Afterward, the hybrid scaffold explored increasing cell adherence, cell proliferation, and compressive strength after implantation because the HA is an inorganic component in human bone providing biocompatible and bioactive properties [15-18].

In addition, the demineralized bone matrix (DBM) is a popular material for scaffolds due to promoting osteoinduction on the scaffold. The DBM is made from decalcification of cortical or spongy bone with acidosis until 2% calcium, collagen type I, and growth factor remains. The DBM approved and classified as a medical device by Food and Drug Administration (FDA) is an alternative allograft and biocompatible material for bone regeneration [19-21]. Previous studies demonstrated successful bone union in 4-6 months after the DBM bone reconstruction. Additionally, the bone scaffold combined with the DBM could promote cell proliferation through osteoinduction and osteoconduction *[22-24]*. Recently, the DBM mixed HA with a 1:3 ratio explored the high significance of osteogenesis after implantation *[25]*. Moreover, the appropriate HA concentration for osteogenesis scaffold ranges from 20-50 % by weight. According to the architecture, interconnected pores of *300-500 µm*, 30-50 % porosity, and pattern with 0°-90° orientations are suitable for osteogenesis scaffolds *[26-36]*. A previous study found that the patterns with 0°-90°, 0°-60°-120°, and 0°-45°-90°-135° orientations showed insignificance in the cell proliferation. They suggested that bone geometry influenced mechanical strength more than cell growth [37].

The synthetic bone in MOWHTO should have the same mechanical strength as the target bone which is a proximal part of the tibial cancellous bone. There is compressive strength ranging from 6-10 MPa. Inadequate mechanical strength leads to critical gab size and instability which relates to the delayed bone union process *[38]*. The scaffold should be concerned with material concentrations and structure according to mechanical compression. Previous research showed that increasing the HA concentrations on PCL demonstrated increased compressive strength in the bone scaffold *[39]*. Likewise, the increasing HA concentrations explored decreased the mechanical strength *[40-41]*. In addition, a popularly architectural scaffold is 0°-90° orientation due to its high strength and easy manufacturing *[37, 42-44]*. However, the effect of DBM-HA combined with PCL concentrations on the compressive strength of bone scaffold substituted in MOWHTO remains inconclusive. Therefore, the study focuses on the compressive strength of bone scaffold with a 1:3 ratio of DBM-HA mixed PCL among 3 concentrations including *20/80, 30/70, and 40/60 % wt./wt. DBM-HA/PCL*. The best concentration providing the highest compressive strength is then utilized to find the mechanical compression of osteogenesis scaffold with *300-500 µm* pore size, 30-50 % porosity, and pattern with 0°-90° orientations for applying with the MOWHTO.

2. *MATERIALS* AND METHODS

In our study, the 3D bone scaffold mimicking had 4 processes: (i) image processing (scaffold design), (ii) materials preparation, (iii) printing, and (iv) mechanical testing. All procedures will be described below. The architectural scaffold is represented in Figure 2.

2.1 Scaffold design

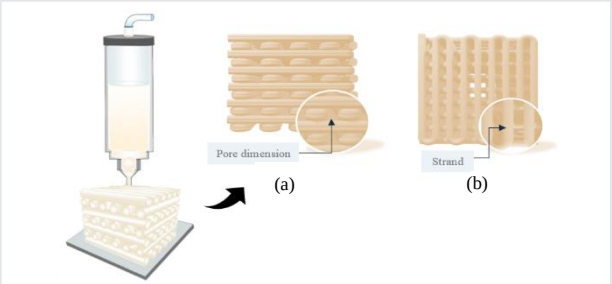

Figure 2. (a) Front view of scaffold architecture and pore dimension and (b) Top view of scaffold architecture and strand

Rectangular specimen preparation

SolidWorks generated the 6×6×12 mm (width×length×height) solid rectangle block for compression test in varied material proportions (Figure 3.). The solid block was sliced with the Perfactory RP program before printing with the bio-plotter. The program generated the layer for 3D printing. The distance between layers is 0.64 mm following the strut dimension.

Cubic specimen preparation

SolidWorks was used to build the STL file of a cubic with dimensions of 10×10×10 mm for compressive testing in structural (0º-90º orientations). After that, the Perfactory RP software cut the block into 16 layers, with 0.64 mm spacing between each layer before printing (Figure 4). A cubic specimen is depicted in Figure 3. The cubic scaffold had a 300-500 µm pore size and 49 % porosity. The porosity of the 0°-90° orientations scaffold was estimated from *equation (1) [45]*.

$$\text{Porosity} = \frac{(F_{dia} \times N_l \times L_2) - ((\frac{F_{dia}}{2})^2 \times \pi \times L \times N_f \times N_l)}{(F_{dia} \times N_l \times L^2)} \times 100 \quad (1)$$

where F_{dia} is the diameter of the filament (mm).
N_l is the number of layers.
N_f is the number of filaments per layer.
L is the length of the scaffold.

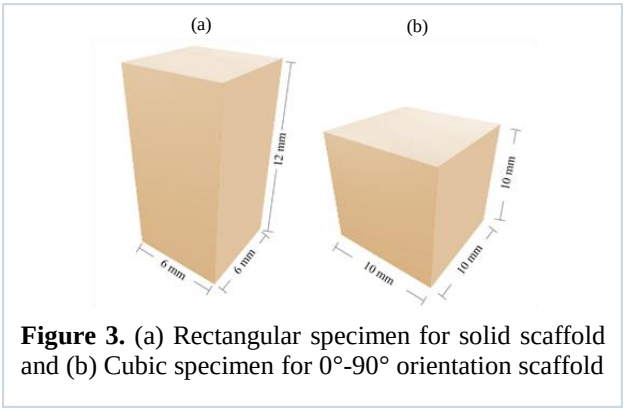

Figure 3. (a) Rectangular specimen for solid scaffold and (b) Cubic specimen for 0°-90° orientation scaffold

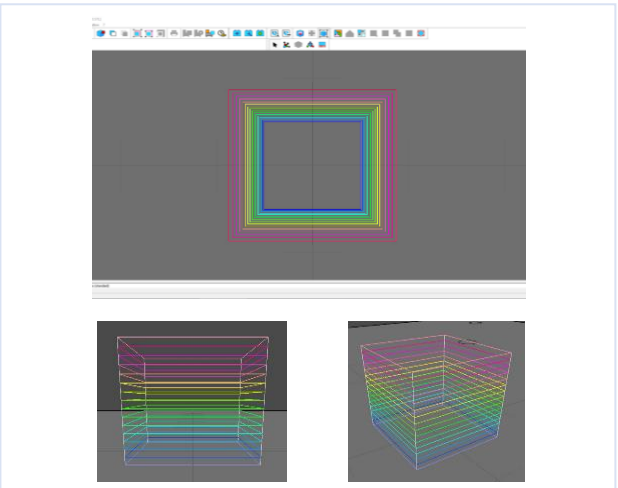

Figure 4. the layers of a 3D model sliced by the RP software

2.2 Material Preparation

Bio-inks for 3D bioprinting were combined with 3 components: (i) the 3 mm PCL pellet (EnvisionTEC PCL 45K RG, Germany, Mw = 90,000 g/mol), (ii) HA powder (CN Lab Nutrition, China, 50 µm particles), and (iii) the 80-100 µm particles DBM powder (Bone & Tissue Bank, King Chulalongkorn Memorial Hospital, Faculty of Medicine Chulalongkorn University, Bangkok, Thailand). The DBM particles were synthesized from the radius and tibia in human bone following King Chulalongkorn Hospital protocols. The DBM and HA were combined with a constant 1:3 ratio. The experiment materials are separated into three distinct groups based on concentrations of 20/80, 30/70, and 40/60 % wt./wt. DBM-HA/PCL. The materials were prepared by melting DBM-HA and PCL at 80-100 °C with magnetic stirring until visibly homogeneous and cut into 2 mm granules in each group *[25]*. Table 1 describes the material concentrations in three groups.

Table 1. Material proportions in 3 groups

Concentration	%wt./wt.		
	DBM	HA	PCL
20/80	5	15	80
30/70	7.5	22.5	70
40/60	10	30	60

2.3 Scaffold fabrication

The bio-plotter (EnvisionTEC™, Bioplotter®, Germany) is used to fabricate the scaffold. The scaffold is printed with an 18G dispensing needle tip, a heated cartridge at 100°C, and a 29°C of the platform. The characteristic of scaffold and printing parameters are shown in Table 2. Figure 5 showed the 3D bio-plotter.

Characteristic scaffold	Nonporous structure	Porous structure (0°-90° orientation)
Pore size (µm)	-	400-500
Porosity (%)	-	48%
Filament diameter (mm)	0.8	0.8
Dispensing velocity (mm/min)	0.6	0.6
Pressure (psi)	0.6	0.6
Temperature platform (°C)	25-30	25-30
Humidity (°C)	35	35

Table 2 Parameter for printing

2.4 Compression Test

The compressive strength test was measured by the ComeTechTM Universal Testing Machine (UTM) which controlled a continuous compression speed at 1 mm/min and applied with 1 kN according to ASTM D695-15. The compressive testing is evaluated until the strain reached 50%. *The compressive stress and strain are calculated by equations (2) and (3). The young's modulus (E) is evaluated from the slope at the initial phase of the stress-strain curve and calculated by equation (4).*

$$\text{Stress } (\sigma) = \frac{F}{A} \tag{2}$$

$$\text{Strain } (\varepsilon) = \frac{\Delta L}{L} \tag{3}$$

where F is the applied force (N).
A is the cross-sectional area (m^2).
ΔL is the change in length (mm).
L is the original length (mm).

$$\text{Young's modulus (E)} = \frac{\sigma}{\varepsilon} \quad (4)$$

where σ is the compressive stress (N/ m^2),
ε is the strain (mm/mm).

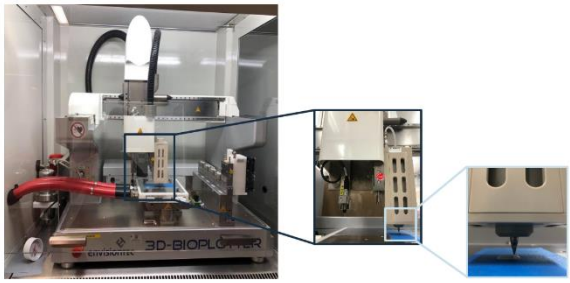

Figure 5. The 3D bio-plotter

STATISTICAL ANALYSIS

The SPSS® program (PASW Statistics for Windows, Version 18.0., Chicago) was used to test the statistical analysis. Shapiro-Wilk test was performed for the evaluation of the data distribution of compressive stress and a compressive modulus. Kruskal-Wallis test was performed to compare compressive stress among three groups and the Mann-Whitney U test for comparison between groups. One-way ANOVA test with Sheff's Post hoc test was performed for comparison compressive modulus. Statistical significance was defined as a p-value below 0.05.

3. RESULT AND DISCUSSION

A solid rectangular scaffold was constructed with18 layers of 0.8 mm strands dimension. The sample was composed of 6 pieces in each group (n = 6). *The compressive strength of 20/80, 30/70, and 40/60 % wt./wt. DBM-HA/PCL concentrations are shown in Figure 6. The compressive modulus of 20/80, 30/70, and 40/60 % wt./wt. DBM-HA/PCL concentrations are represented by the stress-strain curve. Figure 7 shows the compressive modulus.*

The Shapiro Wilk test indicates that the abnormal distributions were significant for 20/80 % wt./wt. DBM-HA/PCL scaffold (W = 0.827, p < 0.001), 30/70 % wt./wt. DBM-HA/PCL scaffold (W = 0.866, p < 0.001), and 40/60 % wt./wt. DBM-HA/PCL scaffold (W = 0.807, p < 0.001). *On the non-parametric analysis, the compressive stress is reported with the median and interquartile ranges (Mdn, Q1-Q3).* According to a Kruskal Wallis test, the variation in DBM-HA mixed PCL concentrations significantly affected the mechanical compressive stress on the bone scaffold (H (2) = 165.65, p < 0.001), with a mean rank of 179.50 for 20/80 % wt./wt. DBM-HA/PCL, 95 for 30/70 % wt./wt. DBM-HA/PCL, and 47 for 40/60 DBM-HA/PCL scaffolds. A Mann-Whitney test indicated that the significant statistic was demonstrated in all paired groups: (i) U ($N_{20/80\ \%\ wt./wt.}$ = 72, $N_{30/70\ \%\ wt./wt.}$ = 72) = 0.000, Z = -10.36, p < 0.001, (ii) U ($N_{20/80\ \%\ wt./wt.}$ = 72, $N_{40/60\ \%\ wt./wt.}$ = 71) = 0.000, Z = -10.32, p < 0.001, and (iii) U ($N_{30/70\ \%\ wt./wt.}$ = 72, $N_{40/60\ wt./wt.}$ = 71) = 786.00, Z = -7.15, p < 0.001. As a result, the compressive stress of DBM-HA/PCL concentrations with 20/80 % wt./wt. (23.25 MPa, 22.39-24.11 MPa) > 30/70 % wt./wt. (17.72 MPa, 15.76-18.76 MPa) > 40/60 % wt./wt. (14.64 MPa, 13.62-15.76 MPa). From the finding, the low DBM-HA concentrations in the PCL group show the high compressive stress and the 20/80 % wt./wt. providing the maximum stress.

The normal distribution of compressive modulus among the 3 groups was performed by the Shapiro Wilk test for 20/80 % wt./wt. DBM-HA/PCL scaffold (W = 0.943, p = 0.683), 30/70 % wt./wt. DBM-HA/PCL scaffold (W = 0.878, p = 0.259), and 40/60 % wt./wt. DBM-HA/PCL scaffold (W = 0.912, p = 0.452). *The one-way ANOVA and Sheff's Post hoc tests were used to compare the three groups.* An analysis of variance showed that the effect of the DBM-HA concentrations in the PCL scaffold on the compressive modulus was a significant difference, F (2,15) = 43.65, p < 0.001. Afterward, Post hoc comparisons were conducted with the Scheffé test indicating that the mean modulus (M) for all groups was significantly different in the various DBM-HA concentrations and the highest modulus was shown in 20/80 % wt./wt. DBM-HA/PCL scaffold (M = 157.63 MPa, SD = 5.12) following 30/70 % wt./wt. DBM-HA/PCL scaffold (M = 118.80 MPa, SD = 16.54), and 40/60 % wt./wt. DBM-HA/PCL scaffold (M = 98.19 MPa, SD = 8.70) respectively.

According to the results, the maximum compressive stress and modulus of the 20/80 % wt./wt. DBM-HA/PCL (23.25 MPa and 157.63 MPa) is consistent with previous research. *Lu et al. [46]* exhibited the ultimate compressive strength of 20/80 % wt./wt. HA/PCL was 25.8 ± 1.1 MPa. They found that incorporation with 20/80 % wt./wt. HA/PCL concentrations showed the most compressive young's modulus and hardness of the HA/PCL scaffolds. *Kim et al. [47] & Huang et al. [48]* studied the biological and mechanical behaviors on the scaffolds with various HA concentrations (0%, 10%, 15%, and 20%). They discovered that the 20% by weight HA composition showed the highest compressive young's modulus due to the higher HA concentration giving the high stiffness particle dispersion on polycaprolactone, which enhanced the scaffold's strengthening. Additionally, *Choi et al. [49]* proposed that the increased inorganic particle in HA on PCL scaffolds significantly improved the mechanical and biological properties of the scaffolds by inducing cell attachment and rigidity. Moreover, the decreased compressive stress and modulus were demonstrated in 30/70 % wt./wt. DBM-HA/PCL (17.72 MPa and 118.80 MPa) and 40/60 % wt./wt. DBM-HA/PCL (14.64 MPa and 98.19 MPa) because of a decrease in PCL concentrations in both groups which resulted in poor mechanical compression.

In comparison to previous studies, several groups observed that a large amount of polycaprolactone (PCL) concentrations not only provided loading support reinforcement but also reduced brittleness *[40-41, 50]*. Furthermore, previous studies explored that over 40 percent weight HA concentrations showed the weakening compressive strength of the scaffolds. They gave the reason that the excessive HA concentrations resulted in poor mechanical strength due to the bonding interruption of PCL chains leading to very brittle *[5, 51-52]*. Our finding suggested that the 20/80 % wt./wt. DBM-HA/PCL providing the highest mechanical compression is the optimal concentration for utilizing bone scaffold construction [53].

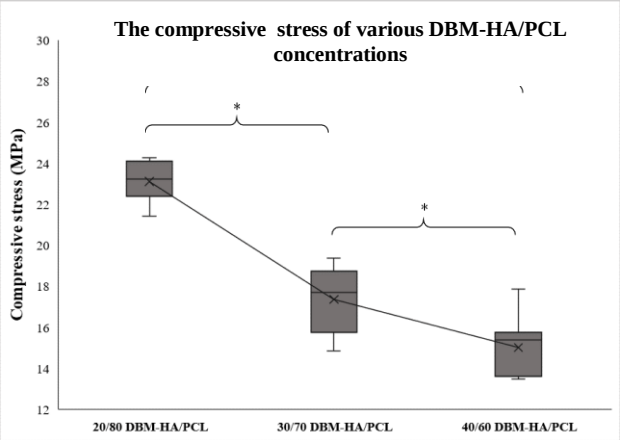

Figure 6. Average of compressive stress was measured at 3 of strain (mm/mm) and compared among difference concentrations of the DBM-HA/PCL (n = 6 of each group). The box graph represented the interquartile of compressive strength and statistical analysis (The Kruskal-Wallis test and a Mann-Whitney test: * $p < 0.05$).

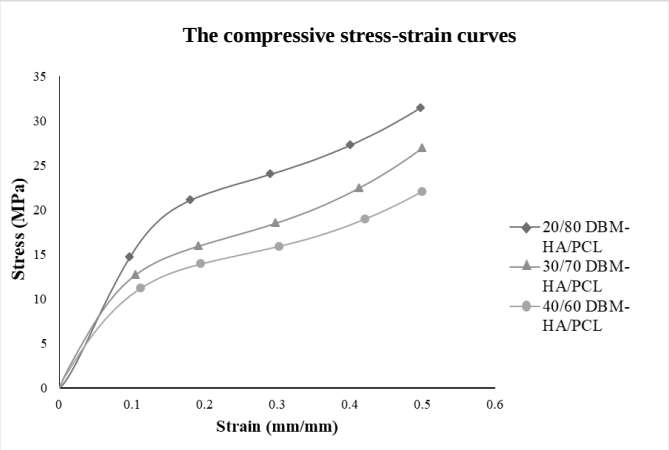

Figure 7. Average of compressive modulus was measured by sloped of stress-strain curves and compared among difference concentrations of the DBM-HA/PCL (n = 6 samples of each group).

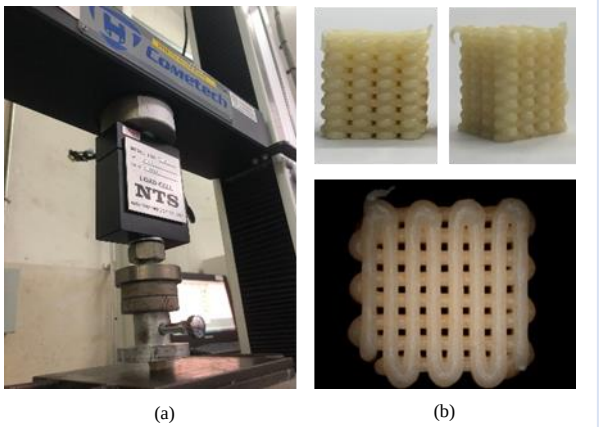

Figure 8. (a) Compression testing with solid and 0°-90° orientations scaffold and (b) A 0°-90° orientations scaffold with 500 µm pore dimension fabricated by the 3D bio-plotter in top and front views.

Table 5. Compressive stress and modulus of a 0°-90° orientations scaffold with 20/80 % wt./wt. DBM-HA/PCL on strains ranging from 0.5 to 4 mm/mm.

Strain (mm/mm)	0°-90° orientations scaffold (n = 5)		
	Compressive stress (MPa)		Compressive modulus (MPa)
	Mdn	Q1-Q3	Mean (SD)
0.05	2.90	1.98 - 4.04	70.92 (10.32)
0.1	6.77	5.67 - 7.75	
0.15	10.00	9.69 - 10.28	
0.2	11.28	10.98 - 12.29	
0.25	12.72	11.77 - 13.07	
0.3	13.81	12.95 - 14.33	
0.35	14.75	13.99 - 15.93	
0.4	16.03	15.20 - 17.65	

Ideally, the MOWHTO synthetic bone must be concerned with biological and mechanical properties. Biological functions represent the bone cell growth within the scaffold. Thus, the MOWHTO DBM-HA/PCL scaffolds were constructed with *a 300-500 µm pore size*, 30-50% porosity, and a pattern with 0°-90° orientations, which the designs allow osteogenesis within the scaffold. In addition, the 20/80 % wt./wt. DBM-HA/PCL was utilized as material to fabricate the scaffold since it provided the highest compressive strength among the three groups. Figure 8 depicts the scaffold's architectural design. Typically, the scaffold should have mechanical properties like natural bone and the target region to avoid delayed bone union process from minimal critical size defection. Several studies showed that the 1.5-2 mm bone gap size allowed for the normal bone healing process while the over 4 mm defect size caused a delayed bone union process *[4, 54-55]*. Thus, the compressive strength was evaluated as less than 0.4 mm/mm of the strain. According to the Shapiro-Wilk test, the compressive

stress of the MOWHTO scaffold showed an abnormal distribution (W = 0.950, p < 0.001), and it was represented in the median and interquartile ranges. The compressive modulus had a normal distribution (W = 0.967, p = 0.856) and was shown in the mean and standard division. The compressive strength and modulus of the MOWHTO scaffold are represented in Table 5.

In previous studies, the compressive stress and modulus in human cancellous bone have ranged from 4-12 MPa and 20-500 MPa *[57-58]*. Additionally, the compressive stress in the tibia trabecular bone ranged from 5.7-7.7 MPa *[59]*. Moreover, the stress distribution in bone after medial open wedge high tibia osteotomy ranged from 5-15 MPa depending on fixation types [*60-61]*. Besides, the ranges of average young's modulus in tibia cancellous bone are 40.12-84.92 MPa *[62]*. According to the finding, the 0°-90° orientations scaffold with 20/80 % wt./wt. DBM-HA/PCL had mechanical compression within the mechanical compression ranging (2.90-16.03 MPa, 70.92 MPa of compressive stress and modulus). However, the osteogenesis scaffold should be considered compressive stress at 0.1-0.15 mm of strain because it results in instability and a narrowing vertical pore dimension after implantation if the scaffold has an excessive strain, and leads to a limitation of the bone union process and bone growth within the scaffold.

From the findings, the scaffold can be used for substitution in the MOWHTO with the tomofix plate because the plate provided the lowest compressive stress on the tibial cancellous bone *[61]*. Moreover, the scaffold with 20/80 % wt./wt. DBM-HA/PCL is necessary to improve mechanical compression because it cannot reach the maximum compressive stress of the tibial cancellous bone after the MOWHTO with other fixations.

To improve mechanical compression, a decrease in pore size and porosity may be a strategy for enhancing the modulus in the MOWHTO scaffolds. Several studies discovered that the increased porosity resulted in poor mechanical strength and decreased compressive modulus [44, 52, 63-64]. Moreover, poor compressive strength was shown in the scaffold with a large pore size [28, 37]. However, the study had numerous drawbacks. Firstly, our study focused on the mechanical compression of the scaffold among three groups of different DBM-HA concentrations in which the DBM-HA is less than the PCL percent by weight. There are undetermined mechanical compression findings of different PCL concentrations in which the DBM-HA is higher than the PCL percent by weight, maybe providing greater mechanical compression because of the influence of high stiff particle concentrations. Secondly, our examination provided the data on mechanical properties without biological properties including cell survival, osteoconduction, and osteoinduction which are important to the scaffold development in the tissue engineering field. Thirdly, the finding represented only the mechanical compression in the 0°-90° orientations which other patterns maybe show better strength. The mechanical simulation will be used in future research to provide the compressive stress of the MOWHTO scaffold. To improve our studies, we will investigate the mechanical compression (concentrations ranging from 20/80, 50/50, and 80/20 % wt./wt. DBM-HA/PCL) and the biological properties (the cell surviving, osteoconduction, and osteoinduction) to determine the optimal concentration providing the highest compressive stress and biological properties.

4. CONCLUSION

This study provides information on the mechanical compression of the difference in DBM-HA/PCL concentrations for the bone tissue engineering field and scientists to improve alternative bone synthesis. According to our study, the various ratios of biphasic scaffolds (DBM-HA/PCL) were successfully fabricated with the bio-plotter. The over concentrations of inorganic particles caused scaffold weakening by PCL bonding interruption and easy brittle of high Ceramic compound. The 20/80 % wt./wt. of DBM-HA/PCL scaffold were suitable ratio and the highest mechanical properties (23.25 MPa and 157.63 MPa respectively). The compressive stress and modulus of the 0º-90º orientations scaffold with 20/80 % wt./wt. DBM-HA/PCL had the 2.90-16.03 MPa and 70.92 MPa respectively which is within the range of trabecular tibia bone in MOWHTO. Finally, the designed scaffold with 0°-90° orientations, 300-500 µm pore size, 49 porosities, and 20/80 % wt./wt. DBM-HA/PCL is accessible for alternative synthetic bone for MOWHTO implantation.

5. ACKNOWLEDGMENT

The authors would like to express their gratitude to the MIND CENTER (Medical Innovations Development Center) at Ramathibodi Hospital and the Bone and Tissue Bank unit at King Chulalongkorn Memorial Hospital for providing me with access to laboratory and research facilities, including the bio-plotter for mimicking scaffolds.

REFERENCES

[1] E. H. Schemitsch, “Size Matters: Defining Critical in Bone Defect Size!,” *J. Orthop. Trauma*, vol. 31, no. 10, pp. S20–S22, 2017, doi: 10.1097/BOT.0000000000000978.

[2] G. Villatte *et al.*, “Opening-wedge high tibial osteotomy with a secure bone allograft (Osteopure™) and locked plate fixation: Retrospective clinical and radiological evaluation of 69 knees after 7.5 years follow-up,” *Orthop. Traumatol. Surg. Res.*, vol. 101, no. 8, pp. 953–957, 2015, doi: 10.1016/j.otsr.2015.09.023.

[3] M. Hudieb *et al.*, “Influence of Age on Calvarial

Critical Size Defect Dimensions: A Radiographic and Histological Study," *J. Craniofac. Surg.*, vol. 32, no. 8, pp. 2896–2900, 2021, doi: 10.1097/scs.0000000000007690.

[4] K. Sato *et al.*, "Establishment of reproducible, critical-sized, femoral segmental bone defects in rats," *Tissue Eng. - Part C Methods*, vol. 20, no. 12, pp. 1037–1041, 2014, doi: 10.1089/ten.tec.2013.0612.

[5] J. H. Han *et al.*, "Is Bone Grafting Necessary in Opening Wedge High Tibial Osteotomy? A Meta-Analysis of Radiological Outcomes," *Knee Surg. Relat. Res.*, vol. 27, no. 4, pp. 207–220, 2015, doi: 10.5792/ksrr.2015.27.4.207.

[6] D. Saragaglia, M. Blaysat, D. Inman, and N. Mercier, "Outcome of opening wedge high tibial osteotomy augmented with a Biosorb® wedge and fixed with a plate and screws in 124 patients with a mean of ten years follow-up," *Int. Orthop.*, vol. 35, no. 8, pp. 1151–1156, 2011, doi: 10.1007/s00264-010-1102-9.

[7] F. R. Noyes, W. Mayfield, S. D. Barber-Westin, J. C. Albright, and T. P. Heckmann, "Opening wedge high tibial osteotomy: An operative technique and rehabilitation program to decrease complications and promote early union and function," *Am. J. Sports Med.*, vol. 34, no. 8, pp. 1262–1273, 2006, doi: 10.1177/0363546505286144.

[8] I. Cristescu *et al.*, "The outcome of tricalcium phosphate wedges used in opening high tibial osteotomy," *Key Eng. Mater.*, vol. 695, no. May, pp. 139–143, 2016, doi: 10.4028/www.scientific.net/KEM.695.139.

[9] S. N. Khan, F. P. Cammisa, H. S. Sandhu, A. D. Diwan, F. P. Girardi, and J. M. Lane, "The biology of bone grafting.," *J. Am. Acad. Orthop. Surg.*, vol. 13, no. 1, pp. 77–86, 2005, doi: 10.5435/00124635-200501000-00010.

[10] W. Wang and K. W. K. Yeung, "Bone grafts and biomaterials substitutes for bone defect repair: A review," *Bioactive Materials*, vol. 2, no. 4. KeAi Communications Co., pp. 224–247, Dec. 01, 2017, doi: 10.1016/j.bioactmat.2017.05.007.

[11] R. Dwivedi *et al.*, "Polycaprolactone as biomaterial for bone scaffolds: Review of literature," *J. Oral Biol. Craniofacial Res.*, vol. 10, no. 1, pp. 381–388, 2020, doi: 10.1016/j.jobcr.2019.10.003.

[12] Y. J. Park, J. H. Cha, S. I. Bang, and S. Y. Kim, "Clinical Application of Three-Dimensionally Printed Biomaterial Polycaprolactone (PCL) in Augmentation Rhinoplasty," *Aesthetic Plast. Surg.*, vol. 43, no. 2, pp. 437–446, 2019, doi: 10.1007/s00266-018-1280-1.

[13] J. H. Kim, G. W. Kim, and W. K. Kang, "Nasal tip plasty using three-dimensional printed polycaprolactone (Smart Ball®)," *Yeungnam Univ. J. Med.*, vol. 37, no. 1, pp. 32–39, 2020, doi: 10.12701/yujm.2019.00290.

[14] S. Lin, "Polycaprolactone facial volume restoration of a 46-year-old Asian women : A case report," no. November 2017, pp. 328–332, 2018, doi: 10.1111/jocd.12482.

[15] E. M. Gonc, F. J. Oliveira, R. F. Silva, M. A. Neto, M. H. Fernandes, and M. Amaral, "Three-dimensional printed PCL-hydroxyapatite scaffolds filled with CNTs for bone cell growth stimulation," pp. 1210–1219, 2015, doi: 10.1002/jbm.b.33432.

[16] P. Chocholata, V. Kulda, and V. Babuska, "Fabrication of Scaffolds for Bone-Tissue Regeneration," 2019, doi: 10.3390/ma12040568.

[17] E. Nyberg, A. Rindone, A. Dorafshar, and W. L. Grayson, "Comparison of 3D-Printed Poly-ϵ-Caprolactone Scaffolds Functionalized with Tricalcium Phosphate, Hydroxyapatite, Bio-Oss, or Decellularized Bone Matrix," *Tissue Eng. - Part A*, vol. 23, no. 11–12, pp. 503–514, 2017, doi: 10.1089/ten.tea.2016.0418.

[18] M. G. Yeo and G. H. Kim, "Preparation and Characterization of 3D Composite Scaffolds Based on Rapid-Prototyped PCL / β -TCP Struts and Electrospun PCL Coated with Collagen and HA for Bone Regeneration," pp. 903–913, 2012, doi: 10.1021/cm201119q.

[19] Zimmer, "Puros ® Demineralized Bone Matrix Brochure," pp. 0–1, 2008.

[20] R. C. Kinney, B. H. Ziran, K. Hirshorn, D. Schlatterer, and T. Ganey, "Demineralized bone matrix for fracture healing: Fact or fiction?," *J. Orthop. Trauma*, vol. 24, no. SUPPL. 1, pp. 52–55, 2010, doi: 10.1097/BOT.0b013e3181d07ffa.

[21] B. Chen *et al.*, "Homogeneous osteogenesis and bone regeneration by demineralized bone matrix loading with collagen-targeting bone morphogenetic protein-2," *Biomaterials*, vol. 28, no. 6, pp. 1027–1035, 2007, doi: 10.1016/j.biomaterials.2006.10.013.

[22] J. B. Mulliken, J. Glowacki, D. Ph, L. B. Kaban, and J. Folkman, "Use of Demineralized Allogeneic Bone Implants for the Correction of Maxillocraniofacial Deformities," pp. 366–372.

[23] G. I. Drosos, P. Touzopoulos, A. Ververidis, and K. Tilkeridis, "Use of demineralized bone matrix in the extremities," vol. 6, no. 2, pp. 269–277, 2015, doi: 10.5312/wjo.v6.i2.269.

[24] P. Torricelli, M. Fini, G. Giavaresi, and R. Giardino, "In vitro osteoinduction of demineralized bone," *Artif. Cells. Blood Substit. Immobil. Biotechnol.*, vol. 26, no. 3, pp. 309–315, 1998, doi: 10.3109/10731199809117461.

[25] J. A. Driscoll *et al.*, "3D-Printed Ceramic-Demineralized Bone Matrix Hyperelastic Bone Composite Scaffolds for Spinal Fusion," *Tissue Eng. - Part A*, vol. 26, no. 3–4, pp. 157–166, 2020, doi: 10.1089/ten.tea.2019.0166.

[26] H. P. Wiesmann and L. Lammers, "Scaffold structure and fabrication," *Fundam. Tissue Eng. Regen. Med.*, pp. 539–549, 2009, doi: 10.1007/978-3-540-77755-7_39.

[27] M. Li, M. J. Mondrinos, X. Chen, M. R. Gandhi, F. K. Ko, and P. I. Lelkes, "Elastin Blends for Tissue Engineering Scaffolds," *J. Biomed. Mater. Res. Part A*, vol. 79, no. 4, pp. 963–73, 2006, doi: 10.1002/jbm.a.

[28] Z. Z. Zhang *et al.*, "Role of scaffold mean pore size in meniscus regeneration," *Acta Biomater.*, vol. 43, pp. 314–326, 2016, doi: 10.1016/j.actbio.2016.07.050.

[29] K. Hayashi, M. L. Munar, and K. Ishikawa, "Effects of macropore size in carbonate apatite honeycomb scaffolds on bone regeneration," *Mater. Sci. Eng. C*, vol. 111, no. March, p. 110848, 2020, doi: 10.1016/j.msec.2020.110848.

[30] M. Stoppato *et al.*, "Influence of scaffold pore size on collagen i development: A new in vitro evaluation perspective," *J. Bioact. Compat. Polym.*, vol. 28, no. 1, pp. 16–32, 2013, doi: 10.1177/0883911512470885.

[31] E. Tsuruga, H. Takita, H. Itoh, Y. Wakisaka, and Y. Kuboki, "Pore size of porous hydroxyapatite as the cell-substratum controls BMP-induced osteogenesis," *J. Biochem.*, vol. 121, no. 2, pp. 317–324, 1997, doi: 10.1093/oxfordjournals.jbchem.a021589.

[32] C. M. Murphy, M. G. Haugh, and F. J. O'Brien, "The effect of mean pore size on cell attachment, proliferation and migration in collagen-glycosaminoglycan scaffolds for bone tissue engineering," *Biomaterials*, vol. 31, no. 3, pp. 461–466, 2010, doi: 10.1016/j.biomaterials.2009.09.063.

[33] S. M. Mantila Roosa, J. M. Kemppainen, E. N. Moffitt, P. H. Krebsbach, and S. J. Hollister, "The pore size of polycaprolactone scaffolds has limited influence on bone regeneration in an in vivo model," *J. Biomed. Mater. Res. - Part A*, vol. 92, no. 1, pp. 359–368, 2010, doi: 10.1002/jbm.a.32381.

[34] F. Liu *et al.*, "Osteogenesis of 3D printed macro-pore size biphasic calcium phosphate scaffold in rabbit calvaria," 2019, doi: 10.1177/0885328218825177.

[35] A. C. Jones, C. H. Arns, D. W. Hutmacher, B. K. Milthorpe, A. P. Sheppard, and M. A. Knackstedt, "The correlation of pore morphology, interconnectivity and physical properties of 3D ceramic scaffolds with bone ingrowth," *Biomaterials*, vol. 30, no. 7, pp. 1440–1451, 2009, doi: 10.1016/j.biomaterials.2008.10.056.

[36] Q. L. Loh and C. Choong, "Three-dimensional scaffolds for tissue engineering applications: Role of porosity and pore size," *Tissue Eng. - Part B Rev.*, vol. 19, no. 6, pp. 485–502, 2013, doi: 10.1089/ten.teb.2012.0437.

[37] M. Domingos *et al.*, "The first systematic analysis of 3D rapid prototyped poly(ε-caprolactone) scaffolds manufactured through BioCell printing: The effect of pore size and geometry on compressive mechanical behaviour and in vitro hMSC viability," *Biofabrication*, vol. 5, no. 4, 2013, doi: 10.1088/1758-5082/5/4/045004.

[38] S. K. Stewart, "Fracture non-union: A review of clinical challenges and future research needs," *Malaysian Orthop. J.*, vol. 13, no. 2, pp. 1–10, 2019, doi: 10.5704/MOJ.1907.001.

[39] S. Eshraghi and S. Das, "Micromechanical finite-element modeling and experimental characterization of the compressive mechanical properties of polycaprolactone-hydroxyapatite composite scaffolds prepared by selective laser sintering for bone tissue engineering," *Acta Biomater.*, vol. 8, no. 8, pp. 3138–3143, 2012, doi: 10.1016/j.actbio.2012.04.022.

[40] J. Zhao, K. Duan, J. W. Zhang, X. Lu, and J. Weng, "The influence of polymer concentrations on the structure and mechanical properties of porous polycaprolactone-coated hydroxyapatite scaffolds," *Appl. Surf. Sci.*, vol. 256, no. 14, pp. 4586–4590, 2010, doi: 10.1016/j.apsusc.2010.02.053.

[41] H. Shao *et al.*, "Effect of PCL concentration on PCL/CaSiO3 porous composite scaffolds for bone engineering," *Ceram. Int.*, vol. 46, no. 9, pp. 13082–13087, 2020, doi: 10.1016/j.ceramint.2020.02.079.

[42] J. Bin Lee, W. Y. Maeng, Y. H. Koh, and H. E. Kim, "Porous calcium phosphate ceramic scaffolds with tailored pore orientations and mechanical properties using lithography-based ceramic 3D printing technique," *Materials (Basel).*, vol. 11, no. 9, 2018, doi:

10.3390/ma11091711.

[43] A. Gleadall, D. Visscher, J. Yang, D. Thomas, and J. Segal, "Review of additive manufactured tissue engineering scaffolds: relationship between geometry and performance," *Burn. Trauma*, vol. 6, no. 1, pp. 1–16, 2018, doi: 10.1186/s41038-018-0121-4.

[44] C. G. Liu, Y. T. Zeng, R. K. Kankala, S. S. Zhang, A. Z. Chen, and S. Bin Wang, "Characterization and preliminary biological evaluation of 3D-printed porous scaffolds for engineering bone tissues," *Materials (Basel).*, vol. 11, no. 10, 2018, doi: 10.3390/ma11101832.

[45] Z. Xu, A. M. Omar, and P. Bartolo, "Experimental and numerical simulations of 3d-printed polycaprolactone scaffolds for bone tissue engineering applications," *Materials (Basel).*, vol. 14, no. 13, Jul. 2021, doi: 10.3390/MA14133546.

[46] L. Lu *et al.*, "Mechanical study of polycaprolactone-hydroxyapatite porous scaffolds created by porogen-based solid freeform fabrication method," *J. Appl. Biomater. Funct. Mater.*, vol. 12, no. 3, pp. 145–154, 2014, doi: 10.5301/JABFM.5000163.

[47] B. Huang, G. Caetano, C. Vyas, J. J. Blaker, C. Diver, and P. Bártolo, "Polymer-ceramic composite scaffolds: The effect of hydroxyapatite and β-tri-calcium phosphate," *Materials (Basel).*, vol. 11, no. 1, 2018, doi: 10.3390/ma11010129.

[48] J. W. Kim, K. H. Shin, Y. H. Koh, M. J. Hah, J. Moon, and H. E. Kim, "Production of poly(ε-caprolactone)/hydroxyapatite composite scaffolds with a tailored macro/micro-porous structure, high mechanical properties, and excellent bioactivity," *Materials (Basel).*, vol. 10, no. 10, 2017, doi: 10.3390/ma10101123.

[49] J. W. Choi, W. Y. Maeng, Y. H. Koh, H. Lee, and H. E. Kim, "3D plotting using camphene as pore-regulating agent to produce hierarchical macro/micro-porous poly(ε-caprolactone)/calcium phosphate composite scaffolds," *Materials (Basel).*, vol. 12, no. 7, 2019, doi: 10.3390/ma12172650.

[50] S. S. Henriksen, M. Ding, M. V. Juhl, N. Theilgaard, and S. Overgaard, "Mechanical strength of ceramic scaffolds reinforced with biopolymers is comparable to that of human bone," *J. Mater. Sci. Mater. Med.*, vol. 22, no. 5, pp. 1111–1118, 2011, doi: 10.1007/s10856-011-4290-y.

[51] H. T. Liao, M. Y. Lee, W. W. Tsai, H. C. Wang, and W. C. Lu, "Osteogenesis of adipose-derived stem cells on polycaprolactone-β-tricalcium phosphate scaffold fabricated via selective laser sintering and surface coating with collagen type I," *J. Tissue Eng. Regen. Med.*, vol. 10, no. 10, pp. E337–E353, Oct. 2016, doi: 10.1002/TERM.1811.

[52] T. R. Kim *et al.*, "Evaluation of structural and mechanical properties of porous artificial bone scaffolds fabricated via advanced TBA-based freeze-gel casting technique," *Appl. Sci.*, vol. 9, no. 9, pp. 1–17, 2019, doi: 10.3390/app9091965.

[53] S. Moeini, M. R. Mohammadi, and A. Simchi, "In-situ solvothermal processing of polycaprolactone/hydroxyapatite nanocomposites with enhanced mechanical and biological performance for bone tissue engineering," *Bioact. Mater.*, vol. 2, no. 3, pp. 146–155, Sep. 2017, doi: 10.1016/J.BIOACTMAT.2017.04.004.

[54] R.-W. Kim, J.-H. Kim, and S.-Y. Moon, "Effect of hydroxyapatite on critical-sized defect," *Maxillofac. Plast. Reconstr. Surg.*, vol. 38, no. 1, pp. 2–7, 2016, doi: 10.1186/s40902-016-0072-2.

[55] R. Meeson, M. Moazen, A. Sanghani-Kerai, L. Osagie-Clouard, M. Coathup, and G. Blunn, "The influence of gap size on the development of fracture union with a micro external fixator," *J. Mech. Behav. Biomed. Mater.*, vol. 99, no. July, pp. 161–168, 2019, doi: 10.1016/j.jmbbm.2019.07.015.

[56] H. A. Zaharin *et al.*, "Effect of unit cell type and pore size on porosity and mechanical behavior of additively manufactured Ti6Al4V scaffolds," *Materials (Basel).*, vol. 11, no. 12, 2018, doi: 10.3390/ma11122402.

[57] S. Yang, K. Leong, Z. Du, and C. Chua, "The design of scaffolds for use in tissue engineering. Part I. traditional factors.," *Tissue Eng.*, vol. 7, no. 6, pp. 679–689, 2001.

[58] S. A. Goldstein, D. L. Wilson, D. A. Sonstegard, and L. S. Matthews, "The mechanical properties of human tibial trabecular bone as a function of metaphyseal location," *J. Biomech.*, vol. 16, no. 12, pp. 965–969, 1983, doi: 10.1016/0021-9290(83)90097-0.

[59] I. Hvid, P. Christensen, J. Søndergaard, P. B. Christensen, and C. G. Larsen, "Acta Orthopaedica Scandinavica Compressive Strength of Tibial Cancellous Bone: Instron® and Osteopenetrometer Measurements in an Autopsy Material," 2009, doi: 10.3109/17453678308992915.

[60] K. T. Kang, Y. G. Koh, J. A. Lee, J. J. Lee, and S. K. Kwon, "Biomechanical effect of a lateral hinge fracture for a medial opening wedge high tibial osteotomy: Finite element study," *J.*

Orthop. Surg. Res., vol. 15, no. 1, pp. 1–10, 2020, doi: 10.1186/s13018-020-01597-7.

[61] Y. G. Koh, J. A. Lee, H. Y. Lee, H. J. Chun, H. J. Kim, and K. T. Kang, "Design optimization of high tibial osteotomy plates using finite element analysis for improved biomechanical effect," *J. Orthop. Surg. Res.*, vol. 14, no. 1, pp. 1–10, 2019, doi: 10.1186/s13018-019-1269-8.

[62] B. Saida, Z. Montassar, S. Dorra, and E. Hamza, "Elasticity Behaviour of a Healthy and Osteoarthritic Human Knee's Fresh Cancellous Bone," *J. Bone Res.*, vol. 06, no. 02, 2018, doi: 10.4172/2572-4916.1000191.

[63] J. P. Gleeson, N. A. Plunkett, and F. J. O'Brien, "Addition of hydroxyapatite improves stiffness, interconnectivity and osteogenic potential of a highly porous collagen-based scaffold for bone tissue regeneration," *Eur. Cells Mater.*, vol. 20, no. 0, pp. 218–230, 2010, doi: 10.22203/eCM.v020a18.

[64] M. Lipowiecki and D. Brabazon, "Design of bone scaffolds structures for rapid prototyping with increased strength and osteoconductivity," *Adv. Mater. Res.*, vol. 83–86, no. January, pp. 914–922, 2010, doi: 10.4028/www.scientific.net/AMR.83-86.914.

Oranich Tangniramai was born in Bankok, Thailand in 1992. She received a B.Sci. in Physical therapy from Mahidol University, Bangkok, Thailand in 2014, Graduate diploma (clinical physical therapy) in 2015 at the same university. Currently, she is studying for a Master's degree in the Department of biomedical engineering, faculty of engineering, Mahidol University of Thailand. Her interests include rehabilitation, the Musculo-skeleton system, and bone 3D printing.

Paweena Diloksumpan received the Doctor of Veterinary Medicine from Chulalongkorn University, Master of Biomedical Engineering from Mahidol University, Bangkok, Thailand. and Ph. D degree in Regenerative Medicine Program, Graduate School of Life Sciences, Faculty of Veterinary Medicine from Utrecht University, the Netherlands. Currently, she works as a researcher in the Biofunctional materials and device research group (BMD) National Metal and Materials Technology Center (MTEC) National Science and Technology Development Agency (NSTDA). Her interests include heart and kidney preservatives, blood pump simulation, and 3D printing.

Chris Charoenlap received the Doctor of Medicine (2nd class honors) and Master of Science (Health Development) from Chulalongkorn University, Bangkok, Thailand. He attended Orthopedic Oncology consultant at King Chulalongkorn Memorial Hospital from 2009 to 2014. After that, He was a lecturer in the faculty of medicine (Department of Orthopedics) at Chulalongkorn University. From 2018 to currently, he works as an Assistant Professor in the Orthopedics department in the faculty of medicine at Chulalongkorn University. His interests include tumors, bone cancer, and artificial bone.

Phornphop Naiyanetr received a B.Eng in Electrical Engineering, an M.Eng in Biomedical Engineering from Mahidol University, Bangkok, Thailand, and a Ph.D. degree in Medical Science in Biomedical Engineering from the Medical University of Vienna, Austria. Currently, he works as an Assistant Professor and director of Cardiovascular engineering and artificial organ laboratory (CardioArt Lab.). His interests include heart and kidney preservatives, blood pump simulation, and 3D printing.